

## Recent earthquakes induced by wastewater disposal near Musreau Lake, Alberta

Tianyang Li<sup>1</sup>, Yu Jeffrey Gu<sup>1</sup>, Jingchuan Wang<sup>1</sup>, Ruijia Wang<sup>2</sup>, Javad Yusifbayov<sup>3</sup>, Mauricio Reyes Canales<sup>3</sup>, and Todd Shipman<sup>3</sup>

<sup>1</sup>Department of Physics, University of Alberta

<sup>2</sup>Department of Earth and Planetary Sciences, University of New Mexico

<sup>3</sup>Alberta Geological Survey, Alberta Energy Regulator

### Summary

Despite a growing number of induced earthquakes in western Canada during the last decade, limited events have thus far been linked to wastewater disposal activity. In this study, we report compelling evidence for the spatiotemporal correlation between the sharply increased earthquakes and four nearby wastewater disposal wells near Musreau Lake, which is the second suspected disposal-induced earthquake swarm in Alberta. Our location and focal mechanism solutions of three tightly spaced clusters from a relocated earthquake catalog (including five local magnitudes > 3) from January 2018 to March 2020 suggest a NNW-SSE trending rupture, during which both poroelastic stress changes and pore fluid diffusion played key roles.

### Introduction

In recent years, increased seismicity has been widely linked to industrial activities in North America. The most common cause of induced events is critically stressed subsurface near high-volume wastewater disposal (WD) wells, as clusters of medium to damaging events have been widely reported in the continental United States (e.g., Hincks et al., 2018). While pressure changes from fluid injection remain the dominant factor, injection wells responsible for induced seismicity in Canada are predominantly associated with hydraulic fracturing (HF) operations during shale gas exploration. Despite a growing number of reports on HF-induced earthquakes in western Canada (e.g., Atkinson et al., 2016), only limited events have thus far been associated with WD activities (Schultz et al., 2014).

On December 25, 2019, an  $M_L$  3.94 earthquake was detected near Musreau Lake (roughly 120 km west of Fox Creek), a region heavily explored for condensate and natural gas liquids but exhibited low susceptibilities to earthquakes prior to 2018. Since then, this region has witnessed substantial growth in water disposal activities and an increased seismicity rate. Three moderate-sized events, with  $M_L$  exceeding 3.5, and their numerous aftershocks raised questions about the criticality of subsurface conditions in this region. The focal mechanisms of these induced earthquakes remain unresolved to date. In this study, we utilize broadband data from several regional seismic networks to investigate the spatiotemporal variations of the Musreau Lake earthquake sequence (from January 2018 to March 2020).

## Data and Methods

The hydrocarbon producing zone in the Musreau lake region is located within the Montney Formation, and the disposal fluids are reinjected into the carbonate reservoir zone. Since June 2017, a cumulative volume (as of March 2020) of  $5 \times 10^6$  m<sup>3</sup> of disposed fluids has been injected into four disposal wells near Musreau Lake.

The seismicity rate increased sharply from January 2018 to March 2020, during which the Alberta Geological Survey reported 48 earthquakes in this region (Figure 1). To construct a comprehensive and accurate catalog of these events, we adopt a machine-learning phase picker (Zhu & Beroza, 2019) to ascertain the P and S arrivals and subsequently refine the absolute event locations by VELEST (Kissling et al., 1994). Finally, we modify a 1-D velocity model based on the inversion of receiver functions and further improve the hypocenter locations using the hypoDD (Waldhauser & Ellsworth, 2000). Our final relocated catalog contains 44 earthquakes with  $M_L > 1.4$  (Figure 2).

To constrain the source further, we utilize high-frequency (0.5-10 Hz) body waves and solve all possible double-couple fault-plane solutions using 1) P, SH, and SV first motion polarities and 2) amplitude information from the rotated three-component seismograms. We are able to determine the focal mechanisms of 40 events with  $M_L$  down to 1.5 (Figure 3).

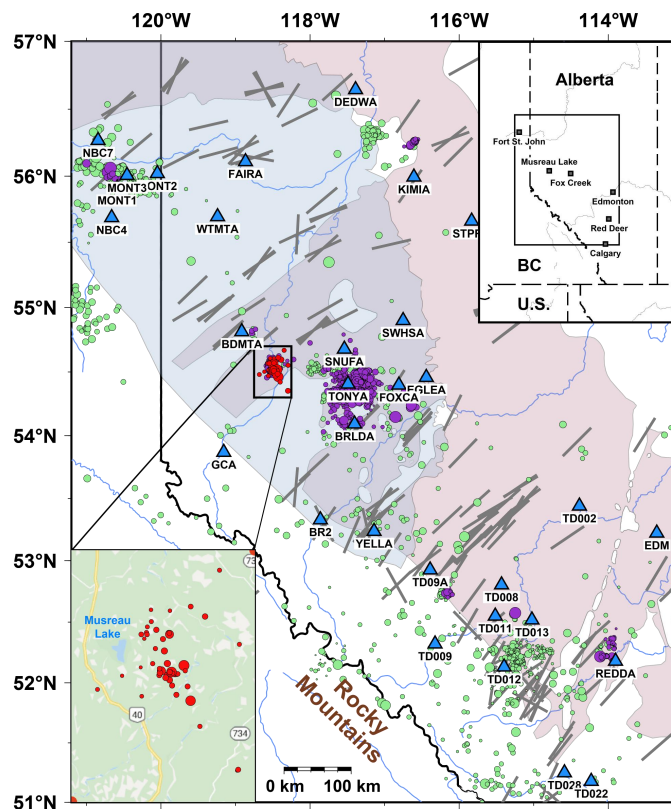


**Fig. 1** Distribution of stations and earthquakes in western Canada (2006-2020). The lower-left corner map shows the earthquake distribution from January 2018 to March 2020 (red circles) in the study region. The magnitude-scaled circles show the natural (green) and induced (purple) earthquakes. The purple and pink-shaded areas show the extent of the Montney and Duvernay Formations. Crustal stress orientations are indicated by the grey lines.

## Spatiotemporal Evolution of the Earthquake Swarm

The proximity of event relocations to the local WD wells, as well as a positive time correlation, favor disposal activity as a potential cause of the increased seismicity. The first earthquake lags the substantially increased injection by about seven months (Figure 2d). This event is followed by periods of significantly increased seismicity during June, September, and December in 2019, which lag the expedited pumping rates by approximately five months, two months, and one month, respectively. We observe a statistically significant correlation between the number of events and the cumulative injection volume over time (Figure 2e). Spatially, most of the relocated events from distinctive clusters are around the four WD injection wells. Starting in June 2019, a continuous increase in injection volume was followed by both a period of increased seismicity and an escalation of event magnitudes.

The relocated hypocenters are spatially more focused on the WD wells than the initial, more spatially variable locations. The hypocenters follow a quasi-linear migration from the northwestern quadrant towards the southeast along a ~10-km-long rupture zone (Figure 2a). The best-fit strike orientation of the rupture area (~45° from North) is roughly parallel to that of the Cordilleran Deformation Front. The depths (Figures 2b and 2c) of most events (5~9 km) are greater than the typical estimates (< 5 km) of possible induced seismic events in western Canada. The source parameters of the earthquakes (Figure 3), which are dominated by NNW-SSE oriented right-lateral strike-slip, are similar to those of regional HF-induced earthquakes (Li et al., 2019).

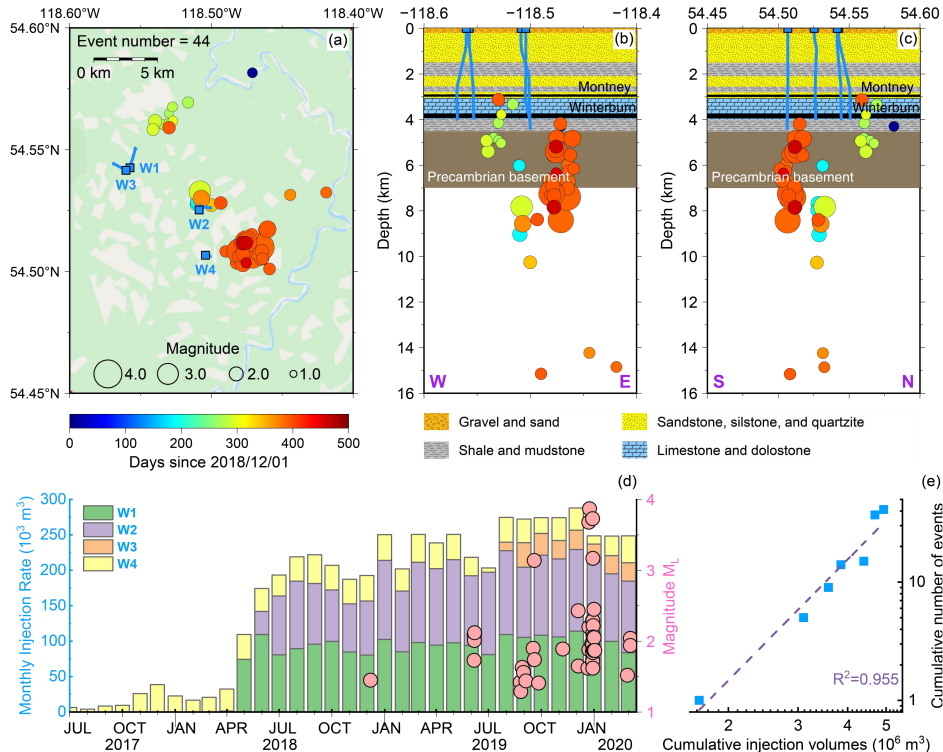


**Fig. 2** Map (a) and cross-sectional (b-c) views of the relocated earthquakes. The four WD wells are shown by the blue lines. (d) Timeline of earthquakes (pink circles) overlaying monthly injection volumes (colored bars). (e) A log-log plot of the cumulative number of events versus cumulative injection volume.

Taken together, the location and source properties suggest three sequential event clusters along the entire fault zone, 1) an early-arriving NW cluster 1 with 3-6 km depths, 2) cluster 2 with hypocentral depths of 6-10 km, and N-S minor normal-faulting components, and 3) a delayed SW cluster (cluster 3) containing four  $M_L > 3$  earthquakes with NNW-SSE fault orientations. Among them, cluster 3 contains over 50% earthquakes of our relocated catalog, including the largest earthquake ( $M_L$  3.94) and three  $M_L > 3$  earthquakes. All events in this cluster occurred within a span of two weeks between 22 December 2019 and 3 January 2020.

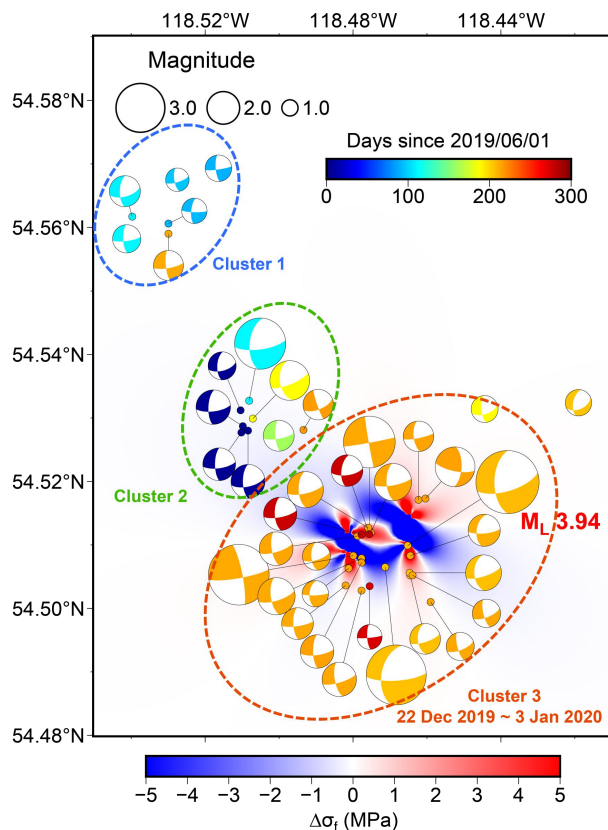


**Fig. 3** A summary of the resolved average double-couple focal mechanisms (scaled by the magnitude and colored by the day of occurrence). The background colors show the Coulomb stress changes ( $\Delta\sigma_f$ ) due to the coseismic slip of the average source parameters.

## Earthquake Triggering Mechanism

In this case, a relatively long delay was required to initiate the seismic activity (cluster 1), while the bulk of the seismic activities (cluster 3) occurred within a subsequent, smaller time window (~1 month). Furthermore, the deeper injections (e.g., well W4) appear to have greater overall impacts on the seismicity. The presence of preexisting faults, which would preferentially diffuse pore pressure into the basement, was commonly suggested for the aforementioned WD-induced earthquakes. However, earthquakes that are sufficiently deeper than the injection zone are unlikely to be triggered by pore pressure diffusion alone. Therefore, other earthquake triggering mechanisms should be considered.

Since most earthquakes in Musreau Lake are located within the crystalline basement, where hydraulic conductivity has likely less impact on fault reactivation, alternative mechanisms such as poroelastic effects could play a major role. Coulomb stress modeling (Figure 3) further suggests that fault slip is potentially promoted by the poroelastic stress changes, which, at least partially, favors earthquake-earthquake interaction via static stress transfer as the primary of the spatiotemporal clustering of the earthquake sequence. Without further constraints, we speculate that the combination of poroelastic stress changes and pore fluid diffusion is mainly responsible for the earthquake swarm near Musreau Lake.

## Conclusions

This study investigates the spatiotemporal variations of the sharply increased seismicity near Musreau Lake, Alberta, the second confirmed case of WD-induced earthquake swarm in Alberta. We develop a relocated earthquake catalog from January 2018 to March 2020. The relocated hypocenters exhibit greater spatial affinity to four WD wells than those reported earlier. The spatiotemporal distribution and the focal mechanism solutions suggest the reactivation of NNW-SSE right-lateral strike-slip faults due to both poroelastic stress changes and pore fluid diffusion.

## Acknowledgements

This study is jointly funded by the National Sciences and Engineering Research Council (NSERC), Future Energy Systems (FES) at the University of Alberta and the Alberta Geological Survey.

## References

- Alberta Geological Survey. (2019). *Alberta Table of Formations; Alberta Energy Regulator* (Vol. 36). Cambridge University Press. Retrieved from [https://ags.aer.ca/publications/Table\\_of\\_Formations\\_2019.html](https://ags.aer.ca/publications/Table_of_Formations_2019.html)
- Atkinson, G. M., Eaton, D. W., Ghofrani, H., Walker, D., Cheadle, B., Schultz, R., et al. (2016). Hydraulic Fracturing and Seismicity in the Western Canada Sedimentary Basin. *Seismological Research Letters*, 87(3), 631–647. <https://doi.org/10.1785/0220150263>
- Hincks, T., Aspinall, W., Cooke, R., & Gernon, T. (2018). Oklahoma's induced seismicity strongly linked to wastewater injection depth. *Science*, 359(6381), 1251–1255. <https://doi.org/10.1126/science.aap7911>
- Kissling, E., Ellsworth, W. L., Eberhart-Phillips, D., & Kradolfer, U. (1994). Initial reference models in local earthquake tomography. *Journal of Geophysical Research*, 99(B10), 19635–19646. <https://doi.org/10.1029/93jb03138>
- Li, T., Gu, Y. J., Wang, Z., Wang, R., Chen, Y., Song, T. A., & Wang, R. (2019). Spatiotemporal Variations in Crustal Seismic Anisotropy Surrounding Induced Earthquakes near Fox Creek, Alberta. *Geophysical Research Letters*, 46(10), 5180–5189. <https://doi.org/10.1029/2018GL081766>
- Schultz, R., Stern, V., & Gu, Y. J. (2014). An investigation of seismicity clustered near the Cordell Field, west central Alberta, and its relation to a nearby disposal well. *Journal of Geophysical Research: Solid Earth*, 119(4), 3410–3423. <https://doi.org/10.1002/2013JB010836>
- Waldhauser, F., & Ellsworth, W. L. (2000). A Double-difference Earthquake location algorithm: Method and application to the Northern Hayward Fault, California. *Bulletin of the Seismological Society of America*, 90(6), 1353–1368. <https://doi.org/10.1785/0120000006>
- Wang, J., Li, T., Gu, Y. J., Schultz, R., Yusifbayov, J., & Zhang, M. (2020). Sequential Fault Reactivation and Secondary Triggering in the March 2019 Red Deer Induced Earthquake Swarm. *Geophysical Research Letters*, 47(22). <https://doi.org/10.1029/2020gl090219>
- Zhu, W., & Beroza, G. C. (2019). PhaseNet: a deep-neural-network-based seismic arrival-time picking method. *Geophysical Journal International*, 216(1), 261–273. <https://doi.org/10.1093/gji/ggy423>